

INTEGRATED MODELING AND MAJOR COMPONENTS OF WATER AND HEAT BALANCES IN A PARTIALLY URBANIZED WATERSHED

By

Yangwen JIA

JST Research Fellow, Urban River Division, River Department
Public Works Research Institute, Ministry of Construction
Ashahi 1, Tsukuba, Ibaraki 305-0804, Japan

and

Nobuyuki TAMAI

Professor, Department of Civil Engineering, University of Tokyo
Hongo 7-3-1, Bunkyo-ku, Tokyo 113-8656, Japan

SYNOPSIS

An integrated study of water and heat balances is pursued which adds more detailed heat balance analysis in hydrological modeling. The newly developed model is grid-based and able to model spatially variable water and heat processes with complex land covers. Evapotranspiration and latent heat flux are computed by the Penman-Monteith equation, infiltration excess during heavy rains is simulated by a generalized Green-Ampt model whereas saturation excess during the remaining periods is obtained by balance analysis in unsaturated soil layers. Surface temperature is solved by the Force-Restore method. A two-dimensional simulation is performed for groundwater flow to consider the interactions between neighboring grid cells. Flow routing is conducted by using the kinematic wave method in a one-dimensional scheme. In addition, the subgrid heterogeneity of land use is also taken into consideration by using a nesting method. The model is applied to the middle-reach watershed of the Tama River in Tokyo and it is verified by the observed discharge at the watershed outlet in the three years from 1992 to 1994. The results show that the annual evapotranspiration varies from a minimum of 300mm in urban areas to a maximum of 800mm in forest areas and distributions of water budgets and heat budgets have similar patterns.

Finally a series of sensitivity analyses show the effects of input data and model parameters on annual water and heat balances. It is found that annual evapotranspiration is much more sensitive to solar radiation than to precipitation, which means solar radiation is a limiting factor to annual evapotranspiration in Tokyo's wet climate. It is also found that most of terms in annual water and heat budgets are less sensitive to the leaf area index and initial soil moisture than to the hydraulic conductivity.

INTRODUCTION

Distributed physically based hydrological models take account of spatial variations of all variable and parameters involved in the basic mathematical equations of the water flows for a watershed. In addition, the used parameters are physically measurable. Therefore, they give a detailed and potentially more correct description of the hydrological processes in the watershed than other hydrological models. With more available data, especially with the development of GIS and remote

sensing technology, the study and application of this type of models will surely be promoted. Today, several popular models are of this type, like SHE (see Abbott et al.(1)), IHDM (see Beven et al. (2)) and MIKE SHE (see Refsgaard and Storm (3)) etc.

On the other hand, land surface parameterization deals with the interaction of water, heat and momentum between land-surface and atmospheric boundary layer (ABL). Although the aim of land surface parameterization is to provide boundary conditions to meteorological / atmospheric models like the General Circulation Models (GCMs) initially, it also includes the effect of climate change on water and heat fluxes on land surface nowadays because a two-way land-atmospheric interaction exists. Land surface parameterization schemes have evolved from the earlier so-called bucket scheme (see Manabe (4)) to the Soil-Vegetation-Atmosphere Transfer Schemes (SVATS). In the bucket scheme, a near-surface layer of soil is modeled as a bucket that can be filled by precipitation and emptied by evaporation or by runoff when a bucket is full. Deardorff (5) proposed a parameterization of scheme of heat and water exchanges at the land surface to be used in meteorological models. In his approach, he included the representation of a vegetation layer with its canopy, interacting both with the soil surface and the atmosphere. This model had been followed by several SVATS with various degrees of modification, e.g., BATS model (see Dickinson et al. (6)) and SiB model (see Sellers et al. (7)).

However, hydrological simulation and land surface parameterization have been studied independently in most cases. Most SVATS models adopt oversimplified description of hydrological processes, that is, infiltration and runoff, and neglect the effect of groundwater table on evapotranspiration and runoff. On the other hand, hydrological models have mostly been concerned with runoff production and influence of vegetation is often represented by modification of potential evapotranspiration with empirical methods. Because water cycle and heat cycle are naturally coupled and advancement of this topic is an interdisciplinary scientific issue among hydrology, environmental biology and meteorology, integrated studies of these two fields are urgent and important. Recently, pioneer studies have been observed, for instance, Famiglietti and Wood (8) etc. However, these studies adopt conceptual or empirical models to simulate some hydrological processes and they are applicable only to natural land covers.

In this paper, an integrated study is pursued which adds more detailed heat balance analysis in hydrological modeling. It is constituted of two main parts: 1) model building and application and 2) sensitivity analysis. In the first part, a distributed and physically based model is developed to explain spatially variable water and heat processes with complex land covers, which is not only applicable to natural watershed but also applicable to urbanized watershed. Evapotranspiration and latent heat flux are computed by combining the Penman-Monteith equation (see Monteith (9)) with the Force-Restore method (see Hu and Islam (10)) instead of potential value method. More efficient and reasonable modeling of infiltration is also conducted by using a generalized Green-Ampt model (see Jia and Tamai (11)). In addition, a nesting method (see Avissar and Pielke (12)) which reflects composition of different land uses inside a grid cell is used to consider the subgrid heterogeneity of land use. In the second part, a series of sensitivity analyses are conducted to find out major components of water and heat balances in a partially urbanized watershed.

MODEL BUILDING AND APPLICATION

Vertical Structure inside a Grid Cell

In this study, the partially urbanized watershed with an area of 579 km² is simulated using a grid cell size of 1km by 1km and a time step of 1 hour. It may give rise big error if the land use inside a grid cell was assumed to be uniform. Therefore, a nesting method which reflects composition of different land uses inside a grid cell is used to consider the heterogeneity of land use inside a grid cell. The area average of water and heat fluxes for all land uses in a grid cell is conducted to calculate the averaged fluxes in the grid cell.

The diagram of the model structure inside a grid cell utilized in this study is shown in Fig.1 (a). Land use is at first summarized into 3 groups, namely a water body group, a soil-vegetation group and

an impervious area group. The soil-vegetation group consists of bare soil, tall vegetation (forest or urban trees) and short vegetation (grass or crops). The impervious area group consists of impervious urban cover and urban canopy. For the soil-vegetation group, 8 vertical layers, namely an interception layer, a depression layer, 3 upper soil layers, a transition layer, an unconfined aquifer and a confined aquifer, are included in the model structure.

Water balances in different land uses are connected together by assuming that groundwater storage is same. The water balance equation for a whole grid is as follows

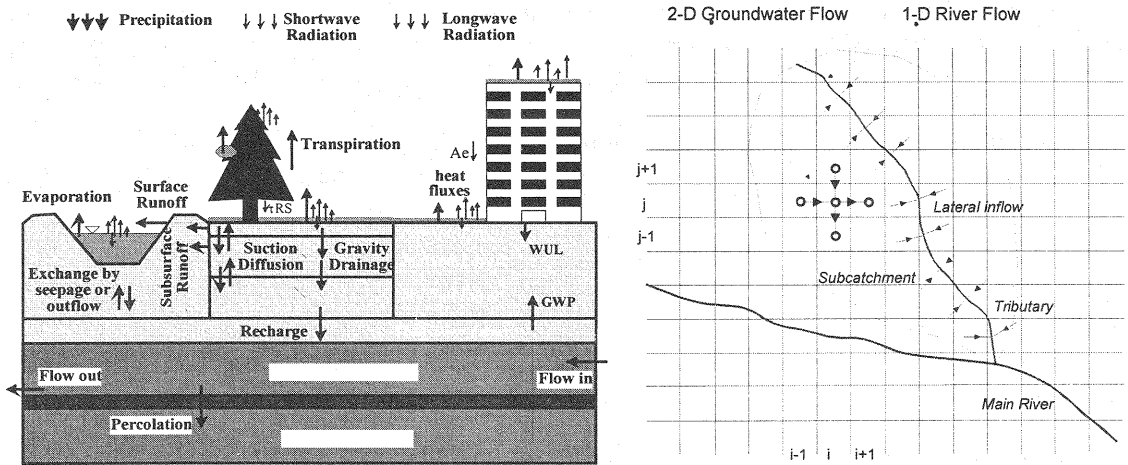
$$P + WUL - GWP = E + R1 + R2 + RG + \Delta S \tag{1}$$

where P is the precipitation, WUL the leakage of water use which is set as 10% of water use based on the Annual Report 1992 by the Department of Water Supply of Tokyo Metropolitan Government, GWP the pumped groundwater, E the evapotranspiration, R1 the surface runoff, R2 the subsurface runoff, RG the groundwater outflow, and ΔS the storage change of unsaturated soil and aquifers.

Heat balance of each land use is also analyzed, respectively. Interaction between soil and vegetation is considered by use of the fraction of transmitted short-wave radiation of vegetation, whereas interaction between urban cover and urban canopy is considered by using the view factor of urban cover. The heat balance equation is as follows:

$$RSN + RLN + Ae = IE + H + G \tag{2}$$

where RSN is the net short-wave radiation, RLN the net long-wave radiation, Ae the artificial energy consumption, IE the latent heat flux, H the sensible heat flux and G the heat conduction into soil.



(a) vertical structure inside a grid cell (b) horizontal structure
 Fig.1 The structure of the proposed model

Horizontal Structure

The interaction among grid cells is considered through two-dimensional groundwater flow in an unconfined aquifer. It is described by the following nonlinear Boussinesq equation:

$$C_u \frac{\partial h_u}{\partial t} = \frac{\partial}{\partial x} (kh_u \frac{\partial h_u}{\partial x}) + \frac{\partial}{\partial y} (kh_u \frac{\partial h_u}{\partial y}) + Q3 + WUL - RG - Per \tag{3}$$

where C_u is the specific yield, h_u the groundwater head in the unconfined aquifer, k the hydraulic conductivity of the unconfined aquifer, Q3 the recharge from unsaturated soil layers, WUL the leakage

of water use, RG the ground-water outflow to rivers and Per the percolation from the unconfined aquifer to the confined aquifer.

River flow routing is conducted for every sub-watershed and a main channel by using the kinematic wave method. Overland flow is simplified as lateral inflow to rivers because the concentration time is estimated to be shorter than the simulation time interval in this study (see Fig.1 (b)).

Hydrological Processes

Evapotranspiration is constituted by 1) interception of vegetation canopies; 2) evaporation from surfaces of waters, soil, urban cover and urban canopy, and from top soil layer; and 3) transpiration from the dry fraction of leaves with the source from the 3 soil layers. The Rutter model (see Rutter and Kershaw (13)) is used to compute interception. The Penman equation is adopted to compute potential evaporation from which actual evaporation from soil is computed using a wetting function. The following Penman-Monteith equation is used to calculate transpiration.

$$E_{PM} = \frac{(RN - G)\Delta + \rho_a C_p \delta_e / r_a}{\lambda[\Delta + \gamma(1 + r_c / r_a)]} \quad (4)$$

where RN is the net radiation, G the heat conduction, Δ the gradient of saturated vapor pressure to temperature, δ_e the air vapor pressure deficit ($e_s - e$), r_a the aerodynamic resistance, r_c the canopy resistance, ρ_a the air density, C_p the air specific heat, λ the latent heat of water and γ the psychrometric constant.

The transpiration is actually supplied from soil layers by roots. A root uptake model is adopted which assumed that the root uptake intensity linearly decreases with the increasing of root depth and the uptake in the upper half root zone accounts for 70% of the total uptake. The transpiration of tall vegetation is assumed to come from the 3 upper soil layers in Fig.1 while that of short vegetation from the 2 upper ones.

Surface runoff of water group is assumed to be the rainfall subtracted by evaporation. In urban group, surface runoff will occur after the depression storage reaches maximum. In soil-vegetation group, it consists of two parts. One is rainfall excess during heavy rain periods computed according to a generalized Green-Ampt model for multi-layered soil with unsteady rainfall. The other is saturation excess in other periods calculated according to water balances in soil layers and unconfined groundwater layers.

Subsurface runoff is computed according to land slope and soil hydraulic conductivity.

Groundwater outflow is estimated by storage function. Outflow coefficient is based on topography and geology (see Ando (14)).

Heat Processes

The net short-wave radiation equals to incoming short-wave radiation subtracted by short-wave reflection. The incoming short-wave radiation is estimated from the sunshine. The net short-wave radiation on each land use is explained as follows after considering the albedo and the sheltering factors:

$$RSN_w = RS(1 - \alpha_w) \quad (\text{water body}) \quad (5)$$

$$RSN_s = RS(1 - \alpha_s)(F_{soil} + \tau_1 \cdot \text{veg1} + \tau_2 \cdot \text{veg2}) \quad (\text{soil}) \quad (6)$$

$$RSN_{v1} = RS(1 - \alpha_{v1})\text{veg1} - RS(1 - \alpha_s) \tau_1 \cdot \text{veg1} \quad (\text{tall vegetation}) \quad (7)$$

$$RSN_{v2} = RS(1 - \alpha_{v2})\text{veg2} - RS(1 - \alpha_s) \tau_2 \cdot \text{veg2} \quad (\text{short vegetation}) \quad (8)$$

$$RSN_{u1} = RS(1 - \alpha_{u1}) Fr \beta \quad (\text{urban cover}) \quad (9)$$

$$RSNu2=RS(1-\alpha u2) (1-Fr \beta) \quad (\text{urban canopy}) \quad (10)$$

$$\text{with } \tau1=\exp(-0.5 LAI1), \quad \tau2=\exp(-0.5 LAI2) \quad (11)$$

where RSN is the net short-wave radiation, α the albedo, $\tau1$ the transmission of short-wave radiation of tall vegetation, $\tau2$ the transmission of short-wave radiation of short vegetation, F_{soil} , $veg1$ and $veg2$ the area fractions of soil, tall vegetation and short vegetation in soil-vegetation group, respectively, LAI the leaf area index, Fr the area fraction of urban cover in impervious area group, and β the view factor of urban cover. Subscripts w , s , $v1$, $v2$, $u1$ and $u2$ denote water body, bare soil, tall vegetation, short vegetation, urban cover and urban canopy, respectively. Except the albedo of water body set as 0.08, those of other land uses are related to solar zenith angle, soil moisture content or canopy heights.

The net long-wave radiation equals to downward long-wave radiation subtracted by upward long-wave radiation, and is related to air temperature and surface temperature. Its expression for each land use is as follows:

$$RLN_w = RLD - RLU_w \quad (12)$$

$$RLN_s = (RLD - RLU_s)F_{soil} + (RLU_{v1} - RLU_s)veg1 + (RLU_{v2} - RLU_s)veg2 \quad (13)$$

$$RLN_{v1} = (RLD + RLU_s - 2RLU_{v1}) veg1 \quad (14)$$

$$RLN_{v2} = (RLD + RLU_s - 2RLU_{v2}) veg2 \quad (15)$$

$$RLN_{u1} = [RLD\beta - RLU_{u1} + RLU_{u2} (1-\beta)] Fr \quad (16)$$

$$RLN_{u2} = RLD(1-Fr\beta) - RLU_{u2}[1-Fr+2Fr(1-\beta)] + RLU_{u1}Fr(1-\beta) \quad (17)$$

$$\text{with } RLD = (1 - (1-\epsilon_{ac}) Fc) \sigma (Ta + 273.2)^4 \quad (18)$$

$$RLU = 0.98 \sigma (Ts + 273.2)^4 \quad (19)$$

$$\epsilon_{ac} = 1 - 0.261 \exp(-7.77E-4 Ta^2) \quad (20)$$

$$Fc = 0.826(Nc)^3 - 1.234(Nc)^2 + 1.135Nc + 0.298 \quad (21)$$

where RLN is the net long-wave radiation, RLD the downward long-wave radiation from atmosphere to land surface, RLU the upward long-wave radiation from land surface to atmosphere, Fc the cloudiness factor, σ the Stefan-Boltzmann constant, ϵ_{ac} the atmosphere emmissivity on clear days, Ta the air temperature, and Ts the land surface temperature.

Statistics of energy consumption indices of 7 types of urban land use are used to consider impacts of human activities on energy balance in urban area. A half of energy consumption is assumed to emit to land surfaces and the other half to air.

Latent heat flux equals to evapotranspiration times the latent heat of water.

Sensible heat flux is computed by the aerodynamic method, namely, it depends on the aerodynamic resistance and the difference between land surface temperature and air temperature.

Heat flux into soil is calculated by using the heat balance Eq.2.

Surface temperature is solved by the Force-Restore method (FRM) with the calculation of coefficient α referred to Hu and Islam which not only ensures minimum distortion of FRM to sinusoidal diurnal forcing but also makes distortion of FRM to higher harmonics negligible.

Study Area and Data Input

The middle-reach watershed of the Tama River is shown in Fig. 2. It is located at the western part of Tokyo Metropolis with an area of 579km². There are 2 discharge stations of the Ministry of Construction, one of which is Chofubashi Station at the upstream inlet of the watershed and the other is Ishihara Station at the outlet of the watershed. Roughly speaking, the region southwest to the Tama

River is dominated by natural streams whereas the region northeast to the Tama River is dominated by a combined sewer system.

Land use data and topography data are based on the Fine Digital Information System (FDIS) of Japan Geography Institute. They are renewed once five years. The land use distribution in 1989 is shown in Fig.3, using a grid resolution of 100m by 100m. It is the newest available data and it is considered to be able to represent the land use in 1992, 1993 and 1994 because urbanization speed is quite low in recent years in the region.

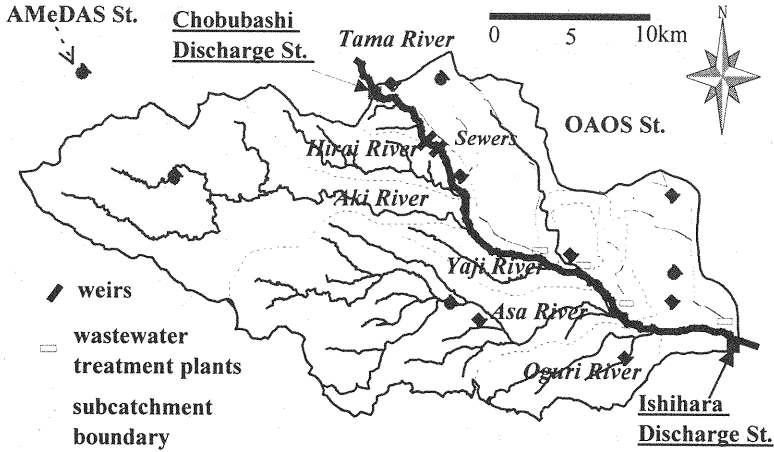


Fig.2 The middle-reach watershed of the Tama River

Soil distribution of top soil layer is shown in Fig.4 which is based on the soil map and the surface geology map made by National Land Bureau of Tokyo Metropolitan Government. Four kinds of soils are considered. Lowland soil distributes in alluvial area along rivers. Brown Forest soil corresponds to western forest area in the watershed, which belongs to Palaeozoic or Mesozoic geological zone. Kanto-loam exists in eastern diluvial tableland zone, which is assumed as urbanized Kanto-loam if urban area fraction is over 0.8. Soils below the top layer are considered as Kanto-loam in the whole watershed. Soil parameters are referred to Herath (15) and Tanimoto (16).

Aquifer parameters are set according to the geology information in every sub-watershed. Roughly speaking, they correspond to two categories, one is Palaeozoic or Mesozoic geological zone with thin aquifers and the other is alluvial or diluvial zone with thick aquifers, though there is a transition zone between them.

The time step is set as 1 hour and the size of every grid cell is set as 1km by 1km in this paper.

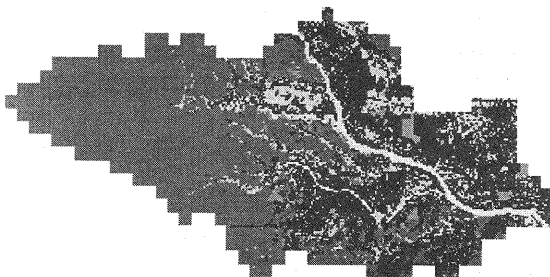


Fig.3 Land use distribution (1989)

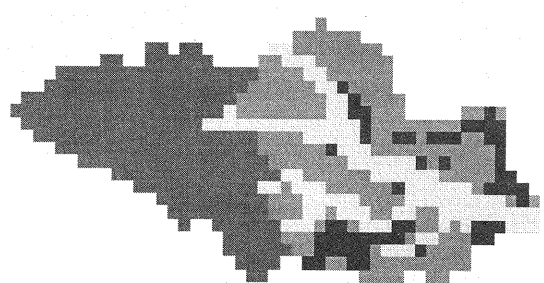


Fig.4 Soil distribution

Calibration and Verification

The calibration of the model is conducted by adjusting various parameters and initial values of soil and aquifer etc. to make the simulated discharge match the observed one at the Ishihara station in 1992. For example, the saturated hydraulic conductivity of Kanto-loam is set as 6.17×10^{-6} m/s, and the outflow coefficient and the initial effective storage are set as 0.012 and 60mm, respectively, for unconfined groundwater in Aki river sub-watershed. The calibrated model is then verified by the observed discharges at the Ishihara station in 1993 and 1994 with all of parameters kept unchanged.

Comparison of daily discharges is shown in Fig. 5. We can see that the simulated discharges are favorably matched with the observed ones. The relative errors of annual average discharges are 1.4 %, 6.6% and 11% in 1992, 1993 and 1994, respectively.

In addition, the deduced inflow into wastewater treatment plants in 1992 by the model is 283 million m^3 , which also matches well with the statistical value of 291 million m^3 .

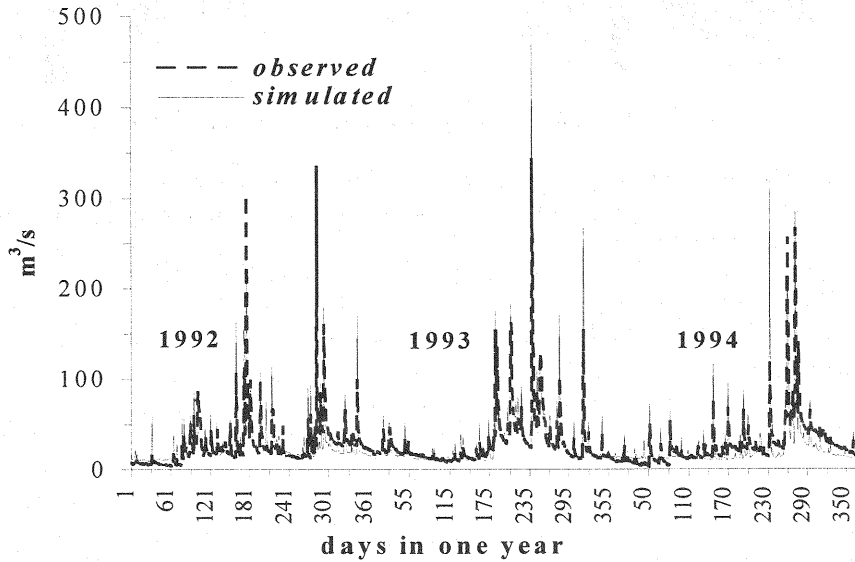


Fig. 5 Daily discharges at Ishihara Station

Annual water and heat balances

Annual water balance and annual heat balance are shown in Tables 1 and 2, respectively. The notations are the same as those in Eqs.1 and 2. Distributions of major components in water and heat budgets in 1992 are shown in Fig.6

Table 1 Annual water balance (mm)

YEAR	P	WUL	GWP	E	R1	R2	RG	ΔS
1992	1555	47	187	630	442	44	306	-7
1993	1494	47	184	638	392	44	315	-32
1994	1423	47	187	710	380	33	213	-54

Table 2 Annual heat balance (MJ/m^2)

YEAR	RSN	RLN	AE	LE	H	G
1992	3549	-1601	149	1548	544	4
1993	3316	-1566	148	1570	326	3
1994	3708	-1606	148	1743	511	-3

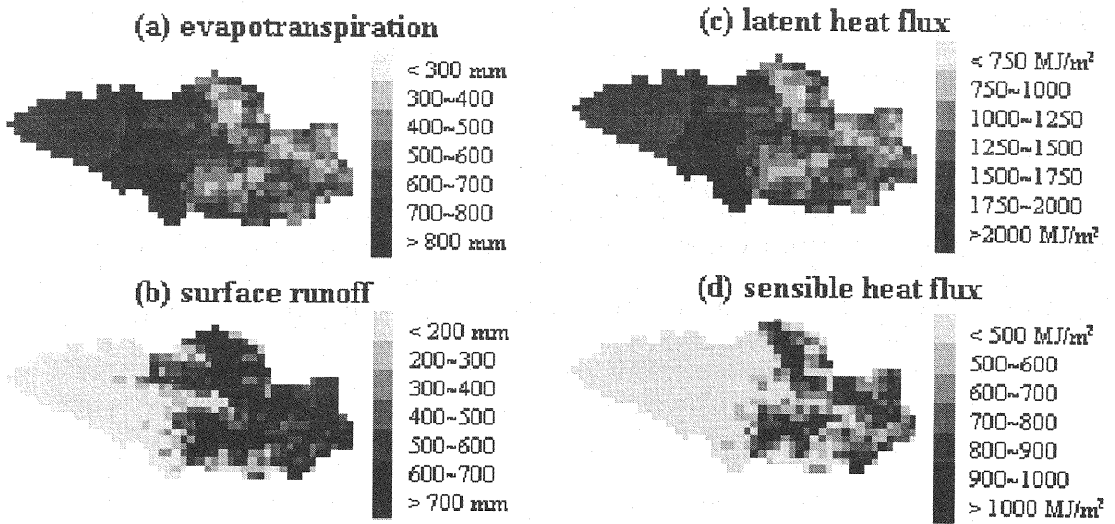


Fig. 6 Distribution of major components in water and heat budgets

From these tables and figures, we can see that: (i) The annual direct runoff ($R1+R2$) coefficient in this watershed is around 0.3, the annual ratio of evapotranspiration to precipitation around 0.4~0.5 and the annual Bowen ratio is around 0.2~0.35. (ii) The annual water and heat budgets vary with years to different extent. For example, in 1994, which was a hot year with a lower annual precipitation compared with 1992, direct runoff and groundwater outflow decreased, whereas evapotranspiration increased because of more solar energy from 1992 levels. (iii) Both water budgets and heat budgets have big spatial variations in the watershed. For example, the annual evapotranspiration varies from a minimum of 300mm in eastern urban areas to a maximum of 800mm in western forest areas, whereas the annual surface runoff has a converse variation. The annual latent heat flux varies from the minimum 750MJ/m² in urban areas to the maximum 2200MJ/m² in forest areas, whereas annual sensible heat flux has a converse variation. (iv) Distributions of relevant components in water budgets and heat budgets show similar patterns. For example, spatial distribution of latent heat flux is similar to that of evapotranspiration and sensible heat flux similar to surface runoff. This shows a close relation between water balance and heat balance.

SENSITIVITY ANALYSIS TO RECOGNIZE MAJOR COMPONENTS

The sensitivity analysis is conducted to see how the model outputs will behave with the change of input data and parameters from the sense of annual and watershed average. In the following part, RN is net radiation ($RN=RSN+RLN+Ae$), I represents infiltration and other notations are the same as those described above.

Effect of Accuracy of Input Data

Two main inputs, incoming solar radiation RS and precipitation are selected to study their effects on major components of annual water and heat budgets in 1992.

Figures 7 and 8 show that (i) the most sensitive to solar radiation RS is sensible heat flux H , (ii) the most sensitive to precipitation P is surface runoff $R1$ and (iii) evapotranspiration E is much more sensitive to solar radiation than to precipitation which means solar radiation is a limiting factor to evapotranspiration in Tokyo where the climate is wet.

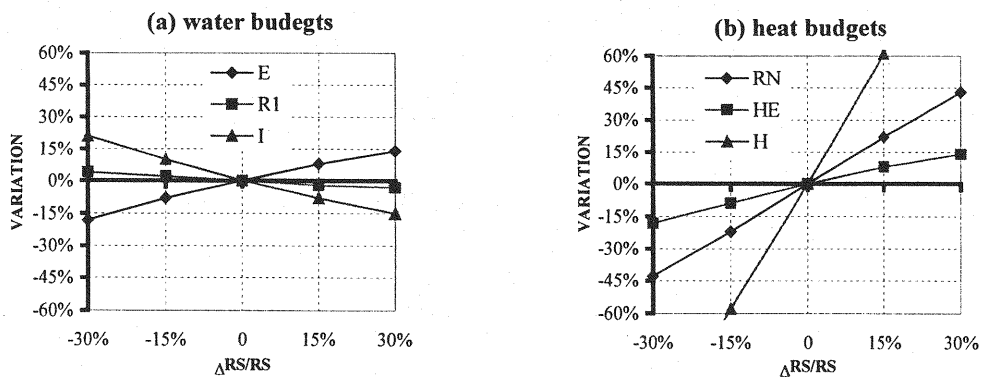


Fig. 7 Effect of incoming solar radiation

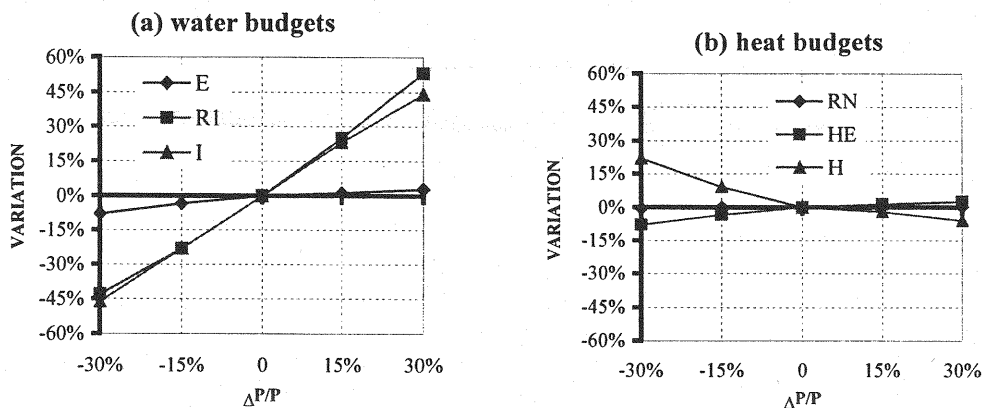
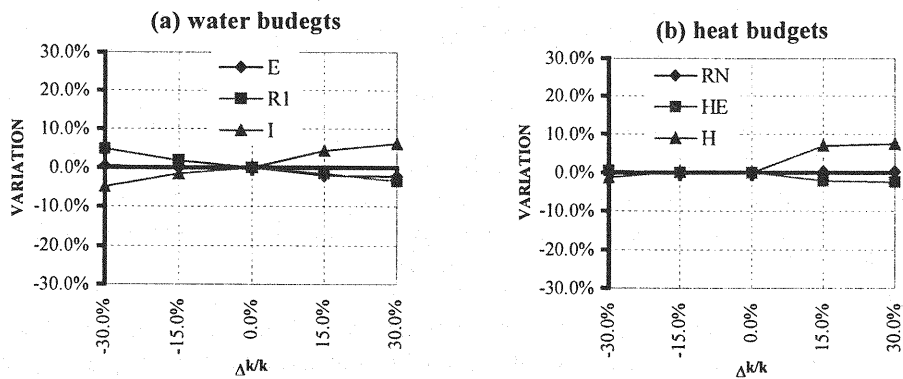


Fig.8 Effect of precipitation

Effect of Variation of Parameters

Two main parameters are studied here, i.e., the saturated hydraulic conductivity k of soil and aquifers and the leaf area index LAI.

From Figs.9 and 10 it can be seen that (i) infiltration I , surface runoff $R1$ and sensible heat flux H are quite sensitive to saturated hydraulic conductivity k and (ii) components of water and heat balance equation are insensitive to the variation of leaf area index LAI and in consequence the annual water and heat budgets are not so sensitive to LAI as to saturated hydraulic conductivity k .

Fig.9 Effect of saturated hydraulic conductivity k

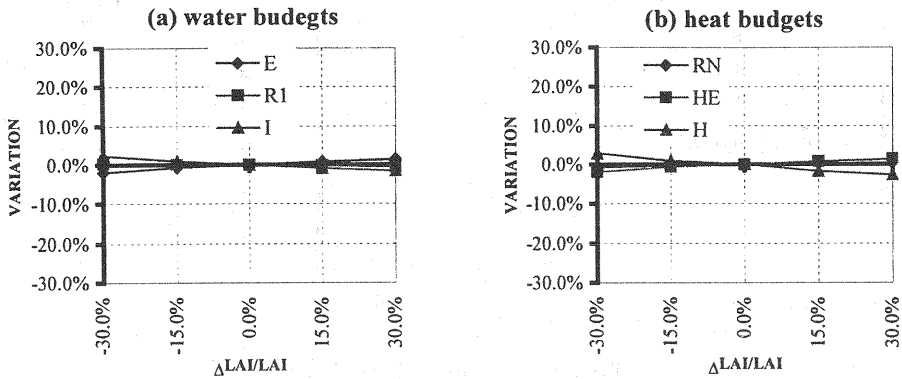


Fig.10 Effect of leaf area index LAI

Effect of Initial Soil Moisture

The effect of initial soil moisture contents of the 3 soil layers is shown on Fig.11. The saturation defined by (soil moisture content - residual moisture content) / (saturated moisture content – residual moisture content) is used for a parameter of initial soil moisture. In the simulation of 3 years described above, the initial soil moisture contents are set as the residual moisture contents because that the soil moisture contents are found approximately equal to the residual values at the end of every year. Although the initial soil moisture contents are found to give some effect on the water and heat budgets of first two months, they have little effect on the annual water and heat budgets except surface runoff R1 and infiltration I (see Fig.11).

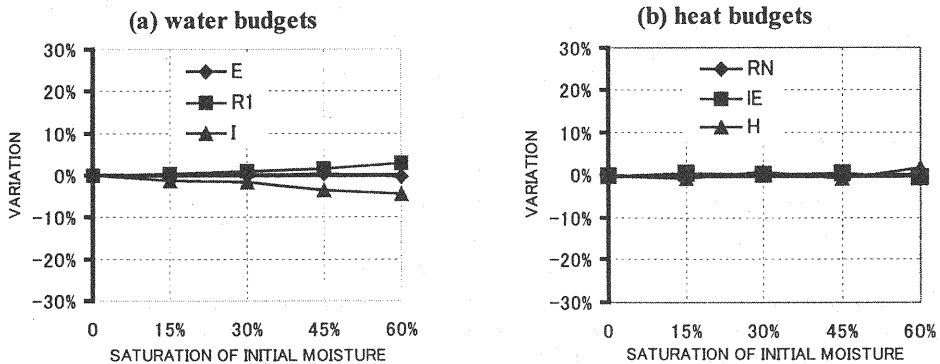


Fig. 11 Effect of initial soil moisture

CONCLUDING REMARKS

Major components of water and heat balances in the middle-reach watershed of the Tama River are made clear through the integrated modeling and the sensitivity analysis. A distributed physically based model is developed taking into account spatially variable water and heat processes with complex land covers. The subgrid heterogeneity of land use is also taken into consideration by using a nesting method. The model is verified by the observed discharge at the watershed outlet in the middle-reach of the Tama River in Tokyo for three years from 1992 to 1994.

It is found that water cycle is closely related to heat cycle and they are impacted simultaneously by the local climate and urbanization. For example, both annual surface runoff and sensible heat flux have a similar uneven distribution pattern because of urbanization, and annual evapotranspiration is much more sensitive to solar radiation than to precipitation because of a wet climate in the watershed.

The sensitivity analysis of parameters shows that most of the annual water and heat budgets are more sensitive to the saturated hydraulic conductivity than to the leaf area index. In addition, the sensitivity analysis of the initial soil moistures shows that they have little effect on most of terms in the annual water and heat budgets except surface runoff and infiltration. Because of the integrated study of water and heat balances, the proposed model is applicable not only to hydrological modeling but also to heat environment analysis.

ACKNOWLEDGMENT

This study is partly supported by A Grant for Strategic Fundamental Research of the Science and Technology Agency (Principal researcher, Prof. M. Sadakata). Thanks are given to Chief Researcher Y. Kawahara (PWRI, MOC), Assistant Professor G. Huang (University of Tokyo) and Chief Engineer H. Matsuzaki (CTI Co. Ltd.) for their valuable comments and assistance in data collection. The authors are also grateful to related departments and institutes of Tokyo Metropolitan Government for their helps in data collection.

REFERENCE

1. Abbott, M. B., J.C. Bathurst, J.A. Cunge, P.E. O'Connell and J. Rasmussen: An Introduction to the European Hydrological System - Systeme Hydrologique Europeen, "SHE", 2: Structure of a physically-based distributed modelling system, *Journal of Hydrology*, 87, 61-77, 1986.
2. Beven K., A. Calver, and E.M. Morris: The Institute of Hydrology Distributed Model, Institute of Hydrology Report 98, Wallingford, UK, 1987.
3. Refsgaard, J.C. and B. Storm: Chapter 23 MIKE SHE in V. J. Singh (Ed) *Computer Models of Watershed Hydrology*, Water Resources Publications, 1113 p., 1995.
4. Manabe, S.: Climate and the ocean circulation: I. The atmospheric circulation and the hydrology of the earth's surface, *Mon. Wea. Rev.*, 97, 739-805, 1969.
5. Deardorff, J. W.: Efficient prediction of ground surface moisture with inclusion of a layer of vegetation, *J. Geophys. Res.*, 20, 1182-1185, 1978.
6. Dickinson, R. E., A Henderson-Sellers, P. J. Kennedy, and M. F. Wilson: Biosphere atmosphere transfer scheme (BATS) for the NCAR community climate model. NCAR/TN-275+STR, National Center for Atmospheric Research, Boulder, CO, 69p., 1986.
7. Sellers, P. J., Y. Mintz, Y. C. Sud and A. Dalcher: The design of a simple biosphere model (SiB) for use within general circulation models, *J. Atmos. Sci.*, 43, 505-531, 1986.
8. Famiglietti, J. S., E. F. Wood: Multiscale modelling of spatially variable water and energy balance processes, *Water Resour. Res.* 30(11), 3061-3078, 1994.
9. Monteith, J. L.: *Principles of Environmental Physics*, Edward Arnold, 236p., 1973.
10. Hu, Z. and S. Islam: Prediction of ground surface temperature and soil moisture content by the force-restore method, *Water Resour. Res.*, Vol.31, No.10, pp.2531-2539, 1995.
11. Jia, Y. and N. Tamai: Modeling infiltration into a multi-layered soil during an unsteady rain, *Ann. J. Hydraul. Eng.*, JSCE, Vol.4sss1, pp.31-36, 1997.
12. Avissar, R. and R. A. Pielke: A parameterization of heterogeneous land-surface for atmospheric numerical models and its impact on regional meteorology, *Mon. Wea. Rev.*, Vol.117, pp.2113-2136, 1989.
13. Rutter, A.J., K. A. Kershaw, P. C. Robins and A. J. Morton: A predictive model of rainfall interception in forests, *Agric. Meteorol.*, Vol.9, pp.367-384, 1971.
14. Ando, Y.: Water cycles in hilly areas and impacts of urbanization (in Japanese), p.254, 1981.
15. Herath, A. S.: Unsaturated zone hydraulic property estimation and applications to infiltration facility analysis, Doctor degree dissertation submitted to Univ. of Tokyo, p.305, 1987.
16. Tanimoto S.: Hydrological modeling for basin management & planning using GIS, Master degree thesis submitted to Univ. of Tokyo (in Japanese), p.75, 1995.

APPENDIX – NOTATION

The following symbols are used in this paper:

A_e	= artificial energy consumption;
C_p	= air specific heat;
C_u	= specific yield;
E	= evapotranspiration;
F_c	= cloudiness factor;
F_{soil}	= area fraction of soil in soil-vegetation group;
F_r	= area fraction of urban cover in impervious area group;
G	= heat conduction into soil;
GWP	= pumped groundwater;
H	= sensible heat flux;
h_u	= groundwater head in the unconfined aquifer;
k	= hydraulic conductivity of the unconfined aquifer;
LAI	= leaf area index;
IE	= latent heat flux;
P	= precipitation;
Per	= percolation from the unconfined aquifer to the confined aquifer;
Q_3	= recharge from unsaturated soil layers;
r_a	= aerodynamic resistance;
r_c	= canopy resistance;
R_1	= surface runoff;
R_2	= subsurface runoff;
RG	= groundwater outflow;
RLD	= downward long-wave radiation from atmosphere to land surface;
RLU	= upward long-wave radiation from land surface to atmosphere;
RLN	= net long-wave radiation;
RSN	= net short-wave radiation;
RN	= net radiation;
T_a	= air temperature;
T_s	= land surface temperature;
$veg1, veg2$	= area fractions of tall vegetation and short vegetation in soil-vegetation group;
WUL	= leakage of water;
δ_e	= air vapor pressure deficit;
Δ	= gradient of saturated vapor pressure to temperature;
ΔS	= storage change of unsaturated soil and aquifers;
α	= albedo;
β	= view factor of urban cover;
γ	= psychrometric constant;
ρ_a	= air density;
λ	= latent heat of water;
σ	= Stefan-Boltzmann constant;
ϵ_{ac}	= atmosphere emissivity on clear days; and
τ_1, τ_2	= transmission of short-wave radiation of tall vegetation and short vegetation.